Macromolecules

Article

pubs.acs.org/Macromolecules

Ion Dispositions in Polyelectrolyte Multilayer Films

Xingjie Zan,[†] David A. Hoagland,[‡] Tian Wang,[†] and Zhaohui Su*,[†]

[†]State Key Laboratory of Polymer Physics and Chemistry, Changchun Institute of Applied Chemistry, Chinese Academy of Sciences, Changchun, 130022, P. R. China

[‡]Polymer Science and Engineering Department, University of Massachusetts Amherst, Amherst, Massachusetts 01003, United States

Supporting Information

ABSTRACT: Polyelectrolyte multilayers (PEMs) fabricated through layer-by-layer (LbL) assembly from sodium chloride-containing solutions of poly(diallyldimethylammonium chloride) (PDDA) and poly(styrene sulfonate) (PSS) were examined by quartz crystal microbalance (QCM), QCM with dissipation (QCM-D), UV−vis spectroscopy, and X-ray photoelectron spectroscopy (XPS) to determine the dispositions of polyelectrolytes and counterions across the PEM thickness. The key experiment was dry film QCM, which by quantifying the incremental mass depositions during LbL assembly uncovered excess polyelectrolyte charge and excess polyelectrolyte charge density as functions of deposition number. Counterion dispositions depended strongly on salt concentration, and trends in the two PEM charge parameters established three salt concentration regimes: zero to near zero salt ([NaCl] $\lesssim$ 0.1 M), low salt (0.1 M $\lesssim$ [NaCl] $\lesssim$ 0.75 M), and high salt ([NaCl] $\gtrsim$ 1.5 M]). The first two are associated with linear LbL growth while the latter is associated with exponential LbL growth. At zero salt, no counterions are present in the PEM bulk (middle), while at low salt, an excess of PDDA charge across the bulk coincides with an excess of counteranions. Differently, at high salt, deposited PSS permeates the PEM bulk, conveying an excess of countercations. At all salt concentrations, the PEM surface charge alternates according to the capping polyelectrolyte's identity. Accumulations of small ions in the PEM bulk can be ascribed to property asymmetries between the two deposited polyelectrolytes, but the roles played by different chain properties remain incompletely understood.

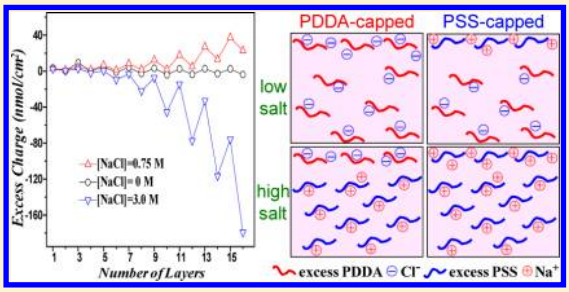

INTRODUCTION

Layer-by-layer (LbL) assembly of oppositely charged polyelectrolytes generates uniform polyelectrolyte multilayers (PEMs) that can be applied as controlled thickness films in optical devices, separation membranes, and drug delivery vehicles.[1−4] PEMs have been prepared from a multitude of polyelectrolyte pairs and under a wide spectrum of growth conditions. Early studies found that, depending on conditions, PEM mass and thickness can rise either linearly or exponentially with the number of deposited layers.[5] The difference suggests the possibility of two (or more) growth modes. LbL growth was also discovered to be virtually athermal, revealing that growth is driven mostly by the entropy gain associated with the release of polyelectrolyte-bound counterions.[6] Counterion identities exert a strong influence over LbL growth and PEM properties,[7−11] most importantly, affecting the incremental masses deposited during assembly as well as the overall PEM thickness. Recently, we discovered that the exchange of PEM-bound counterions followed by their *in situ* reduction offers a facile route to PEM functionalization.[12,13]

The distributions of counterions within PEMs and how these distributions vary with LbL assembly conditions and polyelectrolyte properties remain poorly understood. During assembly, the counterions and polyelectrolytes engage in mutual charge compensation, the ionizable units of a polyelectrolyte neutralized by either the ionizable units of the oppositely charged polyelectrolyte—defining intrinsic compensation—or the small counterions introduced by way of added salt—defining extrinsic compensation.[14] During linear LbL assembly, the fomer is believed to dominate in the middle (or bulk) of a PEM and the latter mainly in the region adjacent to the PEM−solution interface. The presence of counterions in this outermost region is crucial, as the dissociation of small ions from polyelectrolyte provides the surface charge overcompensation necessary for stable LbL assembly. After the first few depositions, the alternating levels of surface charge become constant.[15,16] Although exponential growth is less understood than linear growth, exponential growth is most readily explained as a consequence of the full permeation of one, or both, of the depositing polyelectrolytes across the PEM. If so, to compensate for the charge of the penetrating polyelectrolyte(s), the associated counterions must also distribute across the PEM. While the hypotheses cited here for LbL deposition are not new, some literature clouds the picture, especially in regard to the presence and distribution of counterions. For poly(allylamine hydrochloride)/poly(styrene sulfonate) (PAH/PSS) PEMs made under linear growth, for instance, counterions were reported to distribute across the

Received: July 15, 2012
Revised: October 13, 2012
Published: October 24, 2012

   dx.doi.org/10.1021/ma3014492 | Macromolecules 2012, 45, 8805−8812

PEM bulk.[17−19] Oppositely, as determined by neutron reflectometry, counterions were reported to localize near substrate− and solution−PEM interfaces but not between.[20,21] Other literature suggests that counterion dispositions in PEMs do not depend on growth mode.[22−24] Topological constraints,[15] high binding energy between counterion and polyelectrolyte,[10] Manning condensation,[18] and ability of added ions to form nanocrystals have variously been offered to explain why counterions might reside in the PEM bulk.[17,19]

At least three issues concerning counterions in PEMs thus remain unresolved: (1) the overall concentrations of countercation and counteranion as well as their spatial dispositions across the PEM thickness (and how these concentrations and dispositions depend on salt concentration), (2) why counterions, if present, reside in PEMs, and (3) a systematic means to modulate the counterion presence in PEMs. In this investigation, quartz crystal microbalance (QCM), X-ray photoelectron spectroscopy (XPS), UV−vis spectroscopy, and QCM with dissipation (QCM-D) techniques were chosen to address aspects of these issues, particularly the first, for PEMs constructed across a span of salt concentration.

EXPERIMENTAL SECTION

Materials. PSS (MW ∼ 70 000 g/mol) and PDDA (20 wt % in water, MW ∼ 200 000−350 000 g/mol) were purchased from Aldrich and used as received. Analytical grade sodium chloride (NaCl), *n*-hexane (C_6H_{14}), sulfuric acid (H_2SO_4), ammonia solution ($NH_3{\cdot}H_2O$), hydrogen peroxide (H_2O_2), chloroauric acid ($HAuCl_4$), and ethanol (C_2H_5OH) were purchased from Beijing Chemical Reagents Co. AT-cut quartz crystals with a parent resonant frequency of 9 MHz coated with Ag electrodes were purchased from Beijing Zi Wei Xing Microelectronics, and polished silicon wafers were purchased from Shanghai Wafer Works. Water for both rinsing and preparing solutions was purified by a Millipore Simplicity 185 purification unit (Milli-Q water, resistivity ∼ 18.2 MΩ cm).

Substrate Preparation. Prior to assembly of PEMs on their surfaces, quartz slides and silicon wafers were cleaned for 40 min in 80 °C piranha solution (70:30 v/v H_2SO_4:H_2O_2), rinsed with Milli-Q water, and dried in a stream of N_2. Similarly, gold-coated QCM-D resonators were immersed in an ammonium peroxide mixture [5:1:1 v/v water:$NH_3{\cdot}H_2O$ (25%):H_2O_2 (30%)] at 75 °C, rinsed with water, and dried in a stream of N_2, while QCM crystals were dried after sequential cleanings in *n*-hexane, ethanol, and water for 2 min each.

PEM Preparation. PDDA/PSS PEMs were assembled according to published procedures,[25] which in brief entail alternating 30 min dippings in PDDA (1.0 mg/mL) and PSS (1.0 mg/mL) aqueous solutions containing a specified concentration of NaCl. Except for PEMs to undergo QCM-D characterization, each dipping was followed by a brief rinse in water and then drying in a stream of N_2. PEMs were again dried in a stream of N_2 immediately before PEM characterization. QCM-D characterizations were performed in a continuous flow cell, so the previous rinsing and drying steps were replaced by 5 min rinses with 0.5 M NaCl in the cell. Over the time needed for QCM-D characterization, PEMs suffered no mass loss at this salt concentration. A few PEMs were further functionalized by a 10 min immersion in light-protected 10 mM $HAuCl_4$, a period sufficient for complete exchange of Cl^- for $AuCl_4^-$,[12,13,26,27] and after rinsing and drying, the functionalized PEMs were analyzed by UV−vis immediately.

Quartz Crystal Microbalance (QCM). The 9 mm diameter QCM crystals were coated on each side with circular silver electrodes of 4.5 mm diameter that enabled the resonant frequency change ΔF to be monitored by a Protek frequency counter (Model C3100) and the adsorbed PEM areal mass increment Δm to be deduced from ΔF using the Sauerbrey equation:[28]

$$-\Delta F = \frac{2F_0^2}{A\sqrt{\rho_q \mu_q}}\Delta m \quad (1)$$

where F_0 is the parent crystal resonant frequency (∼9 × 10^6 Hz), A is the electrode area (0.16 cm^2), and ρ_q and μ_q are the density (2.65 g cm^{-3}) and shear modulus (2.95 × 10^{11} dyn cm^{-2}), respectively, of quartz. With the material constants inserted, the Sauerbrey equation simplifies to $-\Delta F = 1.154\Delta m$, when Δm and ΔF are expressed in ng and Hz, respectively. QCM was performed as a series of discrete measurements, where after each deposition the test PEM was rinsed, dried, and measured before immersion in the next polyelectrolyte solution. This protocol was followed three times for all preparation conditions, generating triplicate measurements from which averages and error bars (±1 std dev) are plotted. To confirm the absence of water during QCM characterization, one nominally dry PEM was subject to QCM measurement and then dried for an additional 7 h in a vacuum oven at 60 °C. Afterward, the QCM measurement was repeated, and the mass loss was 1−2%, a negligible correction to the mass changes associated with PEM growth.

Quartz Crystal Microbalance with Dissipation (QCM-D). QCM-D experiments were performed in a Q-sense E1 system, which positions a disk-shaped, AT-cut piezoelectric quartz crystal resonator with deposited gold electrodes inside a fluid cell, where the resonator is excited to oscillation in the thickness shear mode at its fundamental resonant frequency by applying a RF voltage across the electrodes. The cell provides for rapid, nonperturbing exchange of the test liquid exposed to one resonator face, and measurements of ΔF and ΔD for films on this face are accomplished by periodically switching on and off the RF voltage.[29] With soft matter films such as PEMs, a shift ΔF reflects a change in film areal mass Δm (including coupled water), while a shift ΔD bears on changes in frictional (viscous) film losses. The time for a QCM-D measurement is less than 1 s.

X-ray Photoelectron Spectroscopy (XPS). XPS spectra were obtained on a Thermo Electron ESCALAB 250 spectrometer equipped with a monochromatic Al X-ray source (1486.6 eV). The spectra were recorded at a 90° takeoff angle with a 20 eV pass energy.

UV−vis. UV−vis spectra of PEMs constructed on quartz slides were collected on a Shimadzu UV-2450 spectrophotometer.

RESULTS AND DISCUSSION

PEM Mass Growth. Figure 1 plots QCM-derived ΔF against deposition number N for PDDA/PSS PEMs prepared across 0 M ≤ [NaCl] ≤ 3 M. Before each ΔF measurement, a PEM was rinsed and dried, and then with measurement accomplished, the PEM was immersed in the next polyelectrolyte solution to continue to higher N. Even and odd N values

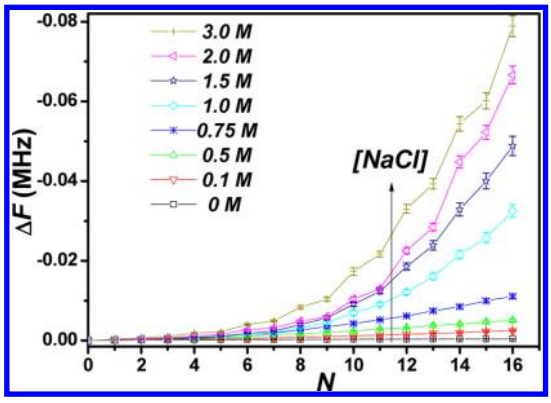

Figure 1. ΔF vs N monitored by QCM during construction of PDDA/PSS PEMs over a span of NaCl concentration. Even N corresponds to PEMs capped by PSS while odd N corresponds to PEMs capped by PDDA.

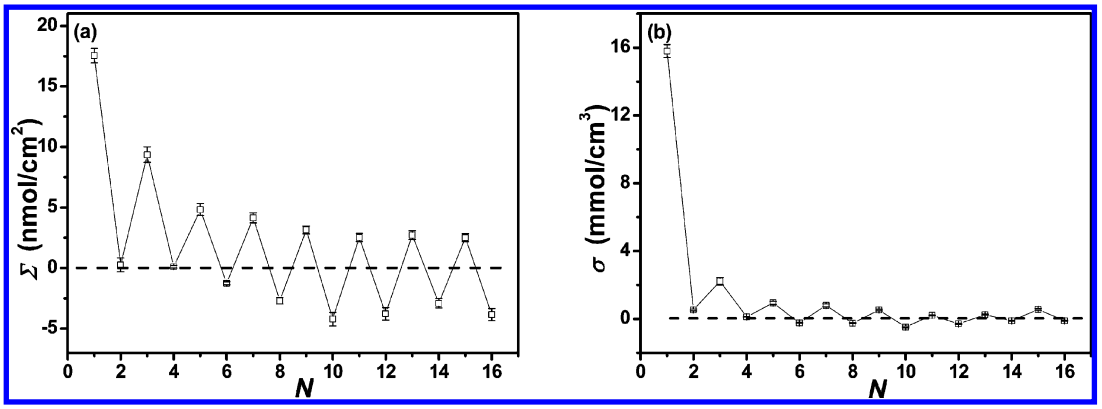

Figure 2. (a) Excess polyelectrolyte charge per area Σ and (b) excess polyelectrolyte charge density σ plotted as functions of deposition number N for PEMs fabricated without NaCl.

thereby correspond to PEMs capped by PSS and PDDA, respectively, and ΔF characterizes the PEM's dry state. Deposition i, where $0 < i \leq N$, contributes to the PEM an areal mass increment Δm^i, with $-\Delta F$ rising continuously with N. Figure 1 shows, as well-known, that areal mass increments are larger at higher salt concentration, leading to thicker PEMs.[30] Ignoring the initial transient ($N \lesssim 4-6$), the overall rise of $-\Delta F$ with N is closely exponential for [NaCl] $\gtrsim$ 1.5 M, while for lower [NaCl] ($\lesssim$0.75 M), where mass increments are smaller and PEMs are thinner, the rise is approximately linear. Careful examination of the growth curves reveals even−odd N oscillations, especially at higher [NaCl], a feature manifesting alternating but unequal successive mass depositions of polycation and polyanion. The monitored trends are in accord with many previous reports on the salt dependence of LbL assembly.[30,31]

Parameters Characterizing PEM Charge. PEMs are essentially charge neutral, so a mismatch in the number of ionizable units between the two polyelectrolytes mandates an excess of one of their counterions. Such mismatches are immediately manifest in the collected QCM data. One QCM-derived PEM charge parameter, the net excess of polyelectrolyte charge per area, Σ, is defined

$$\Sigma = \sum_{i\text{odd}}^{N} \frac{\Delta m^i}{M_{\text{PDDA}}} - \sum_{i\text{even}}^{N} \frac{\Delta m^i}{M_{\text{PSS}}} \qquad (2)$$

where M_{PDDA} and M_{PSS} are the respective PDDA and PSS repeat unit molecular weights (126.2 and 183.2 g/mol, respectively). This formula treats mass depositions as linearly additive. Any loosely bound polyelectrolyte, or any soluble complex created during deposition, would be removed by the water rinse before QCM measurement. UV−vis experiments outlined in the Supporting Information demonstrate that a PDDA deposition negligibly impacts the mass of previously accumulated PSS, arguing that little or no soluble complex is created. Stated differently, PSS desorption is too small to be detected. Further, since the PEMs are dried prior to QCM measurement, differences in hydration ascribable to the capping polyelectrolyte can be ignored. A second and related PEM charge parameter, the excess polyelectrolyte charge density σ, offers a different perspective of the dispositions of charged species

$$\sigma = \frac{\Sigma}{h} = \frac{\Sigma\rho}{m_f} \qquad (3)$$

where h, m_f, and ρ are PEM thickness, areal mass, and density, respectively. For simplicity, and lacking more detailed information, ρ is assigned the arbitrary value 1 g/cm^3. [Dry PSS and PDDA have similar densities, 1.11 and 1.09 g/cm^3, respectively, but the density of their mixture in a dry PEM is unknown. As the form of eq 3 indicates, a small error in ρ propagates as a proportional small error in σ, potentially producing quantitative but not qualitative impacts on σ.]

Salt Concentration Regimes. Salt and polyelectrolyte concentrations, ion and polyelectrolyte identities, and polyelectrolyte molecular weights are among the many variables that affect LbL assembly. Ion and polyelectrolyte identities along with polyelectrolyte molecular weights and concentrations were kept constant throughout this study to focus attention on the influence of salt concentration. Three salt concentration regimes were identified by QCM—zero or near zero salt, low salt, and high salt—and the discussion of experimental results is organized according to regime.

Zero or Near Zero Salt. At zero or near zero salt concentration ([NaCl] $\lesssim$ 0.1 M), flexible polyelectrolytes such as PDDA and PSS adopt extended chain conformations due to the repulsive electrostatic interactions among their chain segments. The LbL assembly of extended polyelectrolytes leads to thin PEMs, the polyelectrolytes deposited in relatively flat conformations. By QCM the PDDA/PSS PEMs made without added NaCl displayed an average bilayer thickness of 0.55 nm ($N > 6$), in reasonable agreement with an average bilayer thickness of 0.46 nm derived by AFM.[32] These thicknesses are comparable to the diameters of the polyelectrolyte backbones but much smaller than the two average dissolved coil sizes. In a salt-free environment, it is not difficult to envisage an incoming polyelectrolyte adopting a conformation that provides effective ion pairing with the oppositely charged polyelectrolytes already at/near the surface and that, as more incoming polyelectrolytes arrive, for the existing surface charge to be erased by the release of nearly all counterions. Figures 2a and 2b plot Σ and σ against N, for zero salt, and both functions oscillate about zero for $N \gtrsim 6$. These dependences establish that, for large enough N, excess polyelectrolyte charge is localized to the PEM surface(s), and the two surface charges become constant. Surface counterions, Na^+ or Cl^-, are so few with zero salt assembly that their detection by XPS proved impossible. Counterions in salt-free PEMs were previously observed, however, by a radio-labeled counterion approach.[16] Substrate influence is well-known for small N PEMs; here, the deposition of PDDA onto the silver QCM electrode creates an

dx.doi.org/10.1021/ma3014492 | Macromolecules 2012, 45, 8805−8812

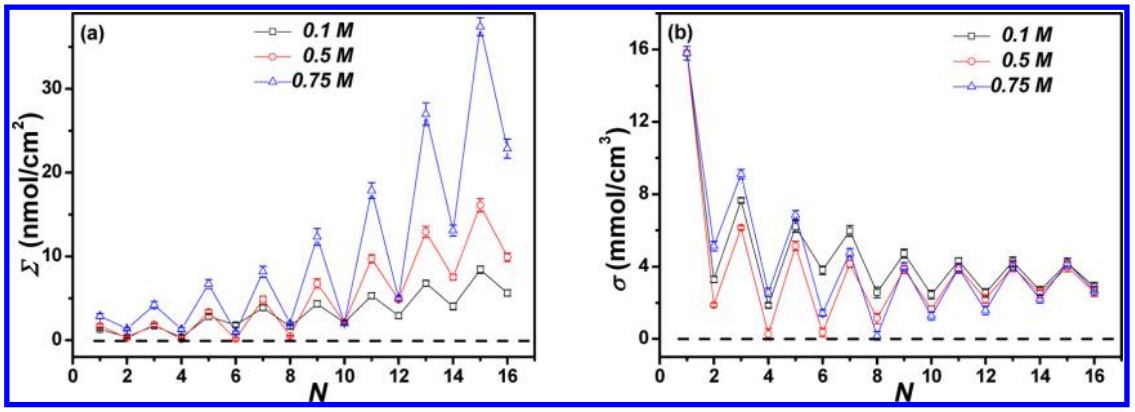

Figure 3. (a) Excess polyelectrolyte charge per area Σ and (b) excess polyelectrolyte charge density σ plotted as functions of deposition number N for PEMs fabricated at three low NaCl concentrations.

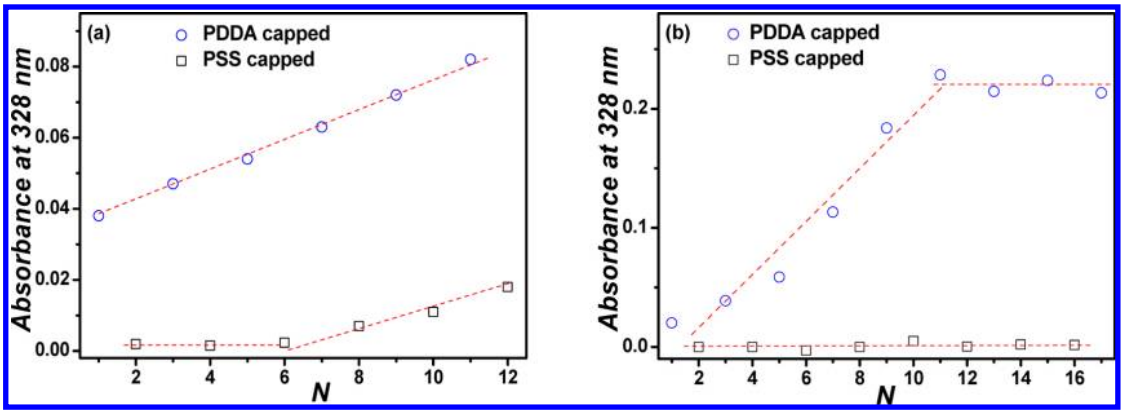

Figure 4. UV absorbance at 328 nm, a quantitative index for $AuCl_4^-$, exchanged into PDDA/PSS PEMs (a) fabricated at [NaCl] = 0.5 M for N odd (i.e., PDDA-capped) and N even (PSS-capped) and (b) fabricated at [NaCl] = 3.0 M for N odd and N even.

initial charge overcompensation too large for neutralization by a single, succeeding PSS layer, and so stable, odd−even oscillations of Σ and σ are found only for $N \gtrsim 6$. When asymptotic behavior is reached, the mean of σ is not perceptibly set away from zero, indicating that the accumulation of counterions in the PEM bulk is negligible.

Low Salt. Figures 3a and 3b exemplify that, for 0.1 M $\lesssim$ [NaCl] $\lesssim$ 0.75 M, a span over which LbL growth remains approximately linear, Σ and σ follow trends different than at zero or near zero salt. Here, while Σ still oscillates with N, a more obvious trend is the large growth of Σ with N, seen for PEMs capped with both PDDA (N odd) or PSS (N even); the growth and accompanying oscillations rise sharply with increasing [NaCl]. Plotted as σ vs N, oscillations superimpose on a slow mean decay that asymptotes to a finite, positive value of σ that is essentially independent of [NaCl]. The rate of decay itself also appears [NaCl] independent.

Slow overall decay of σ to a high N asymptote of finite average value manifests the presence of a constant (i.e., N-independent) density of counterions in the PEM bulk. Indeed, the bulk charge density is given by the asymptote itself, ∼3 mmol/cm^3. Likewise, the diminishing of N oscillations as this asymptotic level is approached illustrates the lessening of the surface contribution to overall polyelectrolyte charge as N rises. As assembly proceeds, the surface charge is simply diluted by a factor of approximately $1/N$ with the bulk charge. Depending on salt concentration, Figure 3a indicates that the bulk charge exceeds the surface charge for $N \gtrsim 10$; the density of charge at the surface is thus much higher than in the bulk. The sharp rise of Σ with [NaCl] noted in Figure 3a after depositions of both PDDA and PSS can thereby be attributed to the growth of Δm^i with increasing [NaCl] and not to other change in the way that the polyelectrolytes deposit. The rate of growth of Σ with N for layers capped with PSS and PDDA are identical, and since PEM growth is linear, so too is the growth of Σ. Since a growing film is dipped, rinsed, dried, and measured repeatedly during QCM characterization, even minor handling errors/artifacts readily compound; meticulous care was crucial to the unmasking of the trends just reported.

In previous reports, we described a counterion exchange method to introduce reducible metal precursor ions into PEMs.[12,13,26,27] The counteranion Cl^-, for example, can exchange with $AuCl_4^-$, an ion detectable in PEMs by its UV−vis absorbance signature. The same ion exchange approach was chosen here to monitor trace levels of Cl^- in the PDDA/PSS PEMs. The difference spectra defined by $AuCl_4^-$ exchange are included in the Supporting Information. The peak at 328 nm, measuring $AuCl_4^-$ incorporation and indirectly reflecting Cl^- content, grows linearly with N for PDDA-capped PEMs, as seen in Figure 4a. A linear dependence is consistent with Cl^- uniformly distributed across the PEM bulk, verifying the QCM finding. The exchange experiment was repeated with PSS-capped PEMs, which would not be expected to possess Cl^- in/on their surfaces. Figure 4a also shows this second experiment's outcome, where at large enough N, a linear increase in peak intensity is again seen. At lower N, the approach detects mainly the Cl^- introduced in the large initial PDDA deposition, which exceeds the Cl^- contributions from

the first few PDDA layers. Apparently, Cl^- resides in the PEM near the substrate for reasons distinct from those operative in the PEM bulk. As noted in the Introduction, others reported counterion accumulations against the substrate.[21] As expected, the lines fit to the high N portions of Figures 4a have almost equal slopes, revealing that the identity of the capping polyelectrolyte does not affect the bulk accumulation of excess polyelectrolyte charge; the QCM data illustrated the same effect.

For PEMs prepared at [NaCl] = 0.5 M, the XPS Cl^- and Na^+ signals for N = 15 and 16 are given in the Supporting Information. In contrast to zero or near zero salt, at this salt concentration Cl^- is detected for both N values while Na^+ is detected for only one, N = 16. Further, the Cl^- intensity for N = 16 is weaker than for N = 15, reflecting the expected impact from capping polyelectrolyte identity. QCM and XPS determinations of ion concentrations are thus consistent, the latter cautioned by the method's smaller signal-to-noise and limited sampling depth, ~5 nm.

Molecular level explanation(s) for Cl^- accumulation in the bulk of PDDA/PSS PEMs at low salt can only be sought in physical or chemical differences between PDDA and PSS chains beyond the sign of their charge units. To shed light on the differences, assembly of PDDA/PSS PEMs at [NaCl] = 0.5 M was monitored by QCM-D. Unlike QCM, QCM-D probes PEMs *in situ* and in real time, and the method provides an additional parameter, ΔD, which integrates mechanical dissipation across the film thickness, including the surface region. Looser and/or more flexible films yield higher ΔD. For N = 12, Figure 5 plots ΔF and ΔD over the time course of LbL

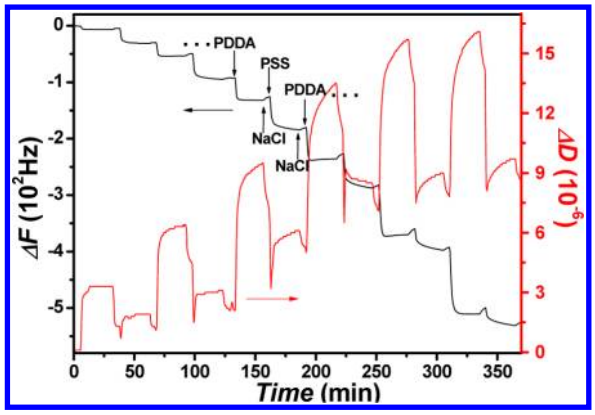

Figure 5. QCM-D shifts of frequency (ΔF) and dissipation (ΔD) plotted against time for PDDA/PSS PEMs fabricated to N = 12 at [NaCl] = 0.5 M. Vertical arrows indicate the beginnings of polyelectrolyte exposures as well as the rinses with NaCl at the ends of polyelectrolyte exposures.

assembly. The evolution of ΔF is familiar from QCM, albeit with parameter magnitudes modulated by the presence of solvent and differences of substrate. Figure 5 reveals odd−even N oscillations in ΔD that demonstrate higher dissipation for PEMs capped with PDDA than those capped with PSS. A PDDA capping layer is therefore looser and/or more extended than a PSS capping layer. From this finding, we speculate that PDDA better conforms to an underlying PSS-capped substrate than vice versa, leading to better ion pairing and greater counterion accumulation. The polyelectrolyte conformational difference can be explained by the greater hydrophobicity of PSS,[33] but other factors, such as chain stiffness, charge density, and molecular weight, could be important.

Beyond the small N region, the σ versus N oscillations of Figure 3b become independent of [NaCl], a feature establishing that the dispositions of counterions (i.e., their bulk and surface densities) depends solely on the properties of the deposited polyelectrolytes. A corollary follows: grown at a constant salt concentration, counterions distribute across the PEM bulk at a concentration dictated by their initial capture at/near the displacing PEM surface. As already discussed, this capture reflects the extent of ion pairing for the polyelectrolyte of deposition N as the oppositely charged polyelectrolyte of deposition N + 1 is attached. Apparently, ion pairing between polyelectrolytes is not much affected by the concentration of salt in the overlying solution. The corollary does not imply that the counterions are themselves layered. The two polyelectrolytes are strongly interpenetrated, and so at the molecular length scale, the counterions must distribute almost evenly across the bulk.

High Salt. Figures 6a and 6b display the dependences of Σ and σ on N for three salt concentrations in the high salt regime ([NaCl] $\gtrsim$ 1.5 M]), which is characterized by exponential PEM growth. Differently than in the earlier salt regimes, at high enough N ($\gtrsim$6−12), an excess accumulation of PSS in the PEM bulk is indicated, coinciding with the presence of Na^+. Since the average σ level at these high N values is [NaCl]-dependent, so too is the bulk density of Na^+, ranging from ~0 to ~3 mmol/cm^3. At lower salt concentrations in this regime, the excess bulk charge density is so low as to make its quantification difficult against the backdrop of odd−even N oscillations due to surface charge. Indeed, at N = 15, the PDDA surface charge still exceeds the PSS bulk charge. (As N grows beyond the range plotted, the bulk charge must eventually dominate.) The constancy of average σ with respective to N in the high N region proves that the local density of polyelectrolyte charge in the PEM bulk is insensitive to PEM thickness. Thus, again, as at low salt, Σ builds with N because the incremental mass depositions are becoming larger, not because the excess charge of the bulk depends on N. These results square with our previous finding that Ag particles formed at high salt concentration by the *in situ* reduction of Ag^+ counterions (introduced by way of ion exchange) are distributed uniformly across the PEM bulk.[13]

For exponentially growing PEMs, several literature reports argue that, rather than remaining at the PEM surface, at least one of the depositing polyelectrolyte species penetrates and crosses the PEM thickness.[37,38] Such transport may well depend on the polyelectrolyte's molecular weight, hydrophobicity, and/or backbone stiffness along with the degree to which the PEM is swollen by salt. For the PEMs under discussion, because an excess negative polyelectrolyte charge accumulates, the penetrating species must be PSS, and from the constancy of σ at high N, PSS permeation must continue to saturation, thereby making the "excess" polyelectrolyte concentration uniform across the PEM bulk. Indeed, polyelectrolyte permeation to saturation supports the proposed mechanism of exponential growth. The thermodynamic impetus for PSS to penetrate deeply into a PEM rather than to reside at/near the PEM surface is uncertain, although a contributing factor could be PSS's relative hydrophobicity.[33] Raising the solution salt concentration is known to swell PEMs,[39] thereby augmenting the rate and extent of polyelectrolyte penetration. At salt concentrations above

dx.doi.org/10.1021/ma3014492 | *Macromolecules* 2012, 45, 8805−8812

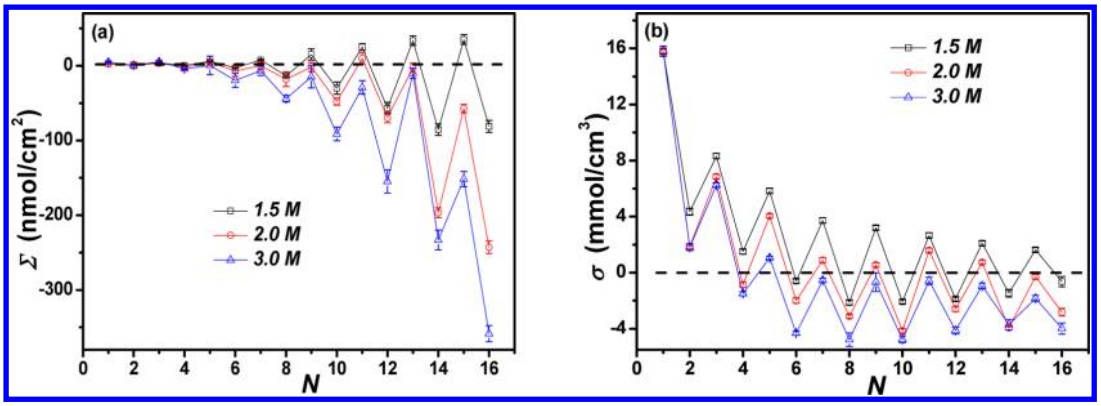

Figure 6. (a) Excess polyelectrolyte charge per area Σ and (b) excess polyelectrolyte charge density σ plotted as functions of deposition number N for PEMs fabricated at three high NaCl concentrations.

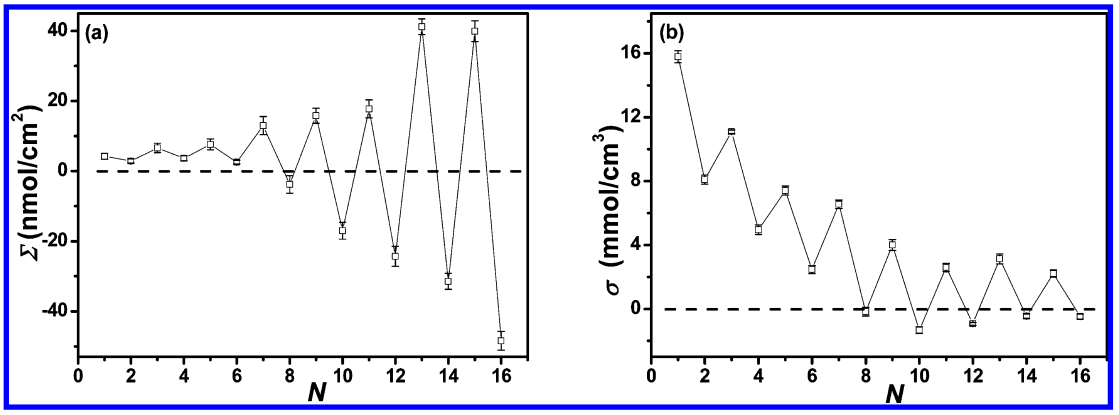

Figure 7. (a) Excess polyelectrolyte charge per area Σ and (b) excess polyelectrolyte charge density σ plotted as functions of deposition number N for PEMs fabricated at [NaCl] = 1.0 M.

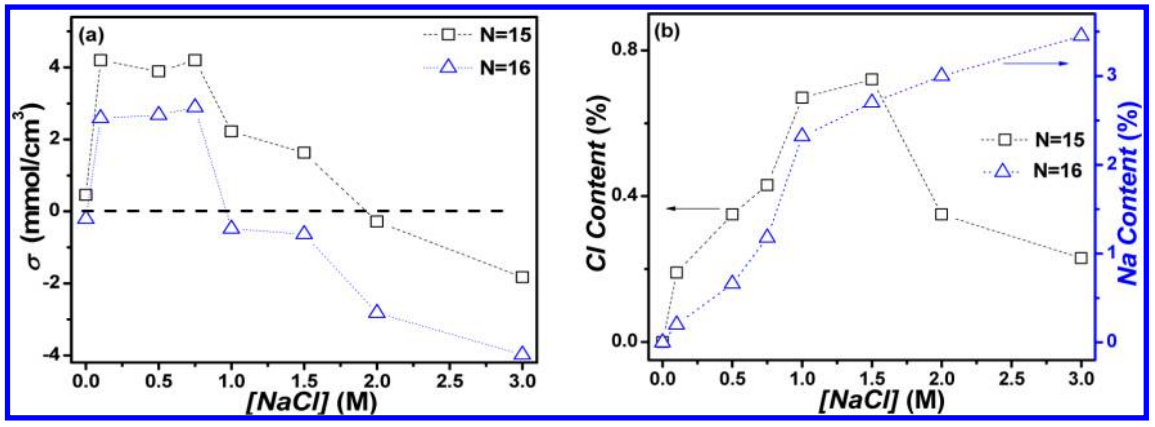

Figure 8. (a) Excess polyelectrolyte charge density σ plotted as a function of [NaCl] for PEMs fabricated at N = 15 (PDDA-capped) and 16 (PSS-capped). (b) Counterion contents (Cl^- for N = 15 and Na^+ for N = 16) in capping layers determined by XPS as functions of [NaCl].

those employed at PEM preparation, however, countercations and counteranions both enter the PEM, complicating analysis of ion and polyelectrolyte dispositions.

Bulk accumulation of mobile PSS at high salt should affect subsequent depositions of PDDA, as ion-pairing with the arriving polycation will drive some of the excess PSS back to the PEM surface region. This back-diffusion should increase incremental mass depositions of PDDA as the PEM grows, raising the film's exponential growth rate. This increased rate of PDDA deposition is evidenced in Figure 6a by the growth of Σ oscillations with N. The same figure shows that at [NaCl] above 2.0 M, Σ remains negative even when PEMs are capped with PDDA. It is the PEM's surface charge that is relevant to the continuation of LbL assembly; the PEM bulk is always charge neutral when all ionic species are considered.

In the high salt regime, conclusions about ion dispositions from UV−vis and XPS are fully consistent with those from QCM. Figure 4b displays trends in the UV−vis absorbance maximum for PDDA-capped PEMs made at [NaCl] = 3.0 M after exchange of Cl^- for $AuCl_4^-$. The absorbance levels off after an initial increase, indicating that counteranions are only present at/near the PEM surface, not in the bulk. XPS (data not shown) monitored the same surface counteranions but failed to detect Na^+, presumably because the ∼25 nm thick PDDA

dx.doi.org/10.1021/ma3014492 | Macromolecules 2012, 45, 8805−8812

cappying layer masks the PEM bulk. Expectedly, for PSS-capped PEMs, XPS detected only Na^+ (data not shown).

Figure 1 sketches a gradual low-to-high salt regime transition, roughly 0.75 M < [NaCl] < 1.5 M, over which growth transforms from linear to exponential. Figures 8a and 8b plot Σ and σ against *N* for a PEM grown in the middle of this transition, at [NaCl] = 1.0 M, and beyond initial growth, both plots display oscillations about zero. Applying the same reasoning as before, these oscillations evidence complete charge overcompensation at each deposition. Indeed, except for a longer initial growth phase, behaviors at 1.0 M seemingly are analogous to those observed at zero or near zero salt, but obviously, the underlying physics are more complex. While more PDDA is deposited than PSS in the capping layer (making σ positive), PSS uptake into the PEM bulk is now significant (driving σ negative), and across the transition, the two phenomena roughly balance, resulting in σ oscillations about zero.

Dependence of σ on [NaCl]. Thus far, the ion dispositions in PEMs have been deduced principally by analyzing plots of Σ or σ against *N*. For the three identified salt regimes, looking beyond the oscillations produced by the capping polyelectrolyte, σ became largely *N*-independent for $N > 5-10$. This limiting σ value provides a key indicator of LbL growth mechanism. Figure 8a plots this value against [NaCl] for $N = 15$ (PDDA-capped) and $N = 16$ (PSS-capped), although *N* has little influence when the capping polyelectrolyte's identity is maintained. The two curves exhibit similar trends: the zero to near zero salt regime is characterized by $\sigma \approx 0$, the low salt regime is characterized by positive and constant σ, and the high salt regime is characterized by increasingly negative σ. The transition from low salt to high salt is gradual, mostly accomplished between 0.75 and 1.5 M, consistent with the analogous transition from linear to exponential LbL growth. Figure 8b displays the XPS-determined surface counterion concentrations (Cl^- for $N = 15$ and Na^+ for $N = 16$) as functions of [NaCl]. For PSS-capping, Na^+ surface content increases monotonically with [NaCl], reflecting greater extrinsic compensation at higher salt.[14] For PDDA capping, Cl^- surface content exhibits a maximum at the low-to-high salt transition. The reduction in Cl^- content at high salt is consistent with PSS diffusion dominating PEM growth; the "back-diffusion" of PSS during PDDA depositions fosters greater intrinsic compensation and exponential growth. The LbL growth mechanism is thereby characteristically imprinted in the way counterions dispose themselves across the PEM bulk.

CONCLUSIONS

Ion dispositions in model PEMs were examined by several experimental approaches, with three salt concentration regimes identified: zero to near zero salt, low salt, and high salt. The first two regimes are associated with linear LbL assembly, and the latter is associated with exponential LbL assembly. Except at special conditions, particularly zero salt, the counterion to one of the polyelectrolytes was found to distribute uniformly across the bulk of the PEM, neutralizing an excess polyelectrolyte charge in this region that increases in proportion to PEM thickness, and a second, thickness-independent population of counterions is found at/near the surface of the PEM, neutralizing the capping polyelectrolyte's excess charge. Careful QCM experiments quantified the localization of counterions within PEMs for the three identified salt regimes: at zero to near zero salt, counterions are present mainly at/near the PEM surface and the bulk of the PEM is counterion-free; at low salt, counterions to one polyelectrolyte species are captured during deposition and remain in the PEM during subsequent LbL assembly, while at the PEM surface, one of the two counterions is present according to the identity of capping polyelectrolyte; and at high salt, one of the polyelectrolyte species penetrates the bulk of the PEM, conveying counterions alongside, while again, one of the counterions is present at/near the surface to neutralize the capping polyelectrolyte. For the PDDA/PSS PEM system, the bulk counterions at low salt are counteranions to PDDA while at high salt they are countercations to PSS; the excess polyelectrolyte charge in the bulk of the PEM is thereby reversed in sign at the initiation of exponential PEM growth. The ion dispositions ultimately reflect property differences between the two polyelectrolytes and how these differences are affected by [NaCl]; here, we speculate that much of the asymmetry can be ascribed to difference in hydrophobicity between PDDA and PSS, although other factors, such as molecular weight and chain stiffness, could be involved. This study's findings buttress speculations in the literature about the reasons for the two LbL growth modes. More importantly, they guide experimental strategies for manipulating ion dispositions within PEMs, strategies needed for PEM functionalization. Although focused on a single PEM system, the principles established in this study should apply to all PEMs fabricated from flexible, highly charged polyelectrolytes deposited from solutions containing simple, symmetric counterions.

ASSOCIATED CONTENT

Supporting Information

UV-vis spectra characterizing the PEM construction process and $AuCl_4^-$ exchanged into the PEM, and XPS spectra for $N = 15$ and 16. This material is available free of charge via the Internet at http://pubs.acs.org.

AUTHOR INFORMATION

Corresponding Author

*Phone (+86)431-85262854; Fax (+86)431-85262126; e-mail zhsu@ciac.jl.cn.

Notes

The authors declare no competing financial interest.

ACKNOWLEDGMENTS

This project was funded by National Natural Science Foundation of China (21174145). Z.S. thanks the NSFC Fund for Creative Research Groups (50921062) for support, and D.A.H. thanks the NSF-funded University of Massachusetts Materials Research Science and Engineering Center for support.

REFERENCES

(1) Decher, G. *Science* **1997**, *277*, 1232.
(2) Decher, G. In *Multilayer Thin Films: Sequential Assembly of Nanocomposite Materials*; Decher, G., Schlenoff, J. B., Eds.; Wiley-VCH: Weinheim, 2003; p 1.
(3) Zhang, X.; Chen, H.; Zhang, H. *Chem. Commun.* **2007**, 1395.
(4) Gribova, V.; Auzely-Velty, R.; Picart, C. *Chem. Mater.* **2012**, *24*, 854.
(5) Lavalle, P.; Gergely, C.; Cuisinier, F. J. G.; Decher, G.; Schaaf, P.; Voegel, J. C.; Picart, C. *Macromolecules* **2002**, *35*, 4458.
(6) Bucur, C. B.; Sui, Z.; Schlenoff, J. B. *J. Am. Chem. Soc.* **2006**, *128*, 13690.

(7) Mermut, O.; Barrett, C. J. *J. Phys. Chem. B* **2003**, *107*, 2525.
(8) Salomäki, M.; Tervasmäki, P.; Areva, S.; Kankare, J. *Langmuir* **2004**, *20*, 3679.
(9) Salomäki, M.; Kankare, J. *Macromolecules* **2008**, *41*, 4423.
(10) Salomäki, M.; Laiho, T.; Kankare, J. *Macromolecules* **2004**, *37*, 9585.
(11) Wang, L.; Lin, Y.; Su, Z. *Soft Matter* **2009**, *5*, 2072.
(12) Zhang, X.; Zan, X.; Su, Z. *J. Mater. Chem.* **2011**, *21*, 17783.
(13) Zan, X.; Su, Z. *Langmuir* **2009**, *25*, 12355.
(14) Schlenoff, J. B.; Dubas, S. T. *Macromolecules* **2001**, *34*, 592.
(15) Caruso, F.; Lichtenfeld, H.; Donath, E.; Möhwald, H. *Macromolecules* **1999**, *32*, 2317.
(16) Schlenoff, J. B.; Ly, H.; Li, M. *J. Am. Chem. Soc.* **1998**, *120*, 7626.
(17) Lourenço, J. M. C.; Ribeiro, P. A.; Botelho do Rego, A. M.; Braz Fernandes, F. M.; Moutinho, A. M. C.; Raposo, M. *Langmuir* **2004**, *20*, 8103.
(18) Riegler, H.; Essler, F. *Langmuir* **2002**, *18*, 6694.
(19) Lourenço, J. M. C.; Ribeiro, P. A.; Botelho do Rego, A. M.; Raposo, M. *J. Colloid Interface Sci.* **2007**, *313*, 26.
(20) Prabhu, V. M.; Vogt, B. D.; Wu, W.-l.; Douglas, J. F.; Lin, E. K.; Satija, S. K.; Goldfarb, D. L.; Ito, H. *Langmuir* **2005**, *21*, 6647.
(21) Tanchak, O. M.; Yager, K. G.; Fritzsche, H.; Harroun, T.; Katsaras, J.; Barrett, C. J. *J. Chem. Phys.* **2008**, *129*, 084901.
(22) Jaber, J. A.; Schlenoff, J. B. *Langmuir* **2007**, *23*, 896.
(23) El Haitami, A. E.; Martel, D.; Ball, V.; Nguyen, H. C.; Gonthier, E.; Labbé, P.; Voegel, J.-C.; Schaaf, P.; Senger, B.; Boulmedais, F. *Langmuir* **2009**, *25*, 2282.
(24) Schlenoff, J. B.; Rmaile, A. H.; Bucur, C. B. *J. Am. Chem. Soc.* **2008**, *130*, 13589.
(25) Wu, G.; Su, Z. *Chem. Mater.* **2006**, *18*, 3726.
(26) Zhang, X.; Chu, C.; Huang, K.; Su, Z. *Chin. J. Appl. Chem.* **2012**, DOI: 10.3724/SP.J.1095.2012.20426.
(27) Zan, X.; Su, Z. *Thin Solid Films* **2009**, *518*, 116.
(28) Serizawa, T.; Yamamoto, K.; Akashi, M. *Langmuir* **1999**, *15*, 4682.
(29) Rodahl, M.; Hook, F.; Krozer, A.; Brzezinski, P.; Kasemo, B. *Rev. Sci. Instrum.* **1995**, *66*, 3924.
(30) McAloney, R. A.; Sinyor, M.; Dudnik, V.; Goh, M. C. *Langmuir* **2001**, *17*, 6655.
(31) Liu, G. M.; Zou, S. R.; Fu, L.; Zhang, G. Z. *J. Phys. Chem. B* **2008**, *112*, 4167.
(32) Pallandre, A.; Moussa, A.; Nysten, B.; Jonas, A. M. *Adv. Mater.* **2006**, *18*, 481.
(33) Ramos, J. J. I.; Stahl, S.; Richter, R. P.; Moya, S. E. *Macromolecules* **2010**, *43*, 9063.
(34) Popov, A.; Hoagland, D. A. *J. Polym. Sci., Part B: Polym. Phys.* **2004**, *42*, 3616.
(35) Loh, P.; Deen, G. R.; Vollmer, D.; Fischer, K.; Schmidt, M.; Kundagrami, A.; Muthukumar, M. *Macromolecules* **2008**, *41*, 9352.
(36) Qiao, B.; Cerdà, J. J.; Holm, C. *Macromolecules* **2010**, *43*, 7828.
(37) Lavalle, P.; Picart, C.; Mutterer, J.; Gergely, C.; Reiss, H.; Voegel, J. C.; Senger, B.; Schaaf, P. *J. Phys. Chem. B* **2004**, *108*, 635.
(38) Salomäki, M.; Kankare, J. *J. Phys. Chem. B* **2007**, *111*, 8509.
(39) Zan, X.; Peng, B.; Hoagland, D. A.; Su, Z. *Polym. Chem.* **2011**, *2*, 2581.